Simulation of High-Realistic Multipath Environments: Developments and Applications

Frank Schubert[1,2] and Bernhard Krach[1]

[1]German Aerospace Center (DLR), Institute of Communications and Navigation

Oberpfaffenhofen, 82234 Wessling, Phone: +49 8153 2841, Fax: +49 8152 1871

[2]European Space Agency (ESA/ESTEC/TEC-EEP)

E-Mail: *firstname.lastname*@dlr.de

Abstract

Compared to the various effects which degrade GNSS performance in general, nowadays multipath propagation accounts for the most dominant error in satellite navigation. Other error sources like satellite clock deviation and atmospheric effects for example can be compensated to a certain degree by the use of high-stability timing equipment (as for example the hydrogen maser in GIOVE-B represents), SBAS corrections, multi-frequency Galileo ranging and pilot signals, and the future availability of civil signals with a higher bandwidth than the currently available C/A code signal. Especially in high-multipath environments like urban and suburban areas, the performance of GNSS receivers is severely affected by multipath propagation.

Extensive measurement campaigns were undertaken during the last years by the German Aerospace Center (DLR) for different scenarios such as the aeronautical, vehicular/pedestrian urban, sub-urban and rural environments, to record and model effects caused by multipath signal reception. Based on the measurement campaigns sophisticated high-realistic channel models have been developed in recent years, which allow for the investigation of multipath effects on GNSS receiver performance and which are foreseen as well to support the design and development of future navigation signals and high performance multipath mitigation algorithms.

To advance and push the development of those GNSS applications, which currently still suffer seriously from multipath reception, areas of work at DLR cover all relevant issues related to multipath, reaching from the aforementioned measurement campaigns and the development of high-realistic channel models to subsequent hardware/software simulation of navigation receivers and the development and assessment of novel mitigation algorithms.

After an introduction to the aeronautical and urban GNSS channel models developed by DLR, a newly developed time-domain sample-true GNSS simulation software is introduced. In the subsequent paragraph novel particle-filter based algorithms for multipath mitigation are described. Combining these three components (GNSS channel models – realistic GNSS simulation – particle-filter multipath mitigation) culminates in the assessment of multipath errors in safety-critical applications such as aviation, and the simulation-based verification of

novel receiver signal processing methods as well as the assessment of navigation signals under realistic propagation conditions.

Analysis of Multipath in Aeronautical Environments

In the last years the usage of GNSS for aviation was a quickly growing field. In this context the problem of multipath reception becomes crucial as aviation demands high accuracy navigation based upon GNSS throughout all phases of flight and in particular with strong requirements for the approach and landing phase. To address this issue future aeronautical applications require detailed multipath analyses [14], which can take benefit of the satellite-to-aircraft navigation channel model (SANCM) developed by DLR in 2003 [19], which found its way into the recommendation ITU 682-2 [21]. This section presents the simulated pseudo-range [1] tracking performance of a navigation receiver as function of the satellite azimuth γ and elevation θ (see Figure 1) relative with respect to the aircraft, using the SANCM and a standard receiver model. The presented results are plotted in polar azimuth-elevation plots whose interpretation is corresponding to Figure 1. Due to the SANCM limitations the results cover an elevation range from 10° to 70° and an azimuth range from 10° to 170° and 190° to 350°. The limitations of the angular values arise from the physical optics model that underlies the ASCM, where the fuselage is modelled as a cylinder [19]. Due to that fact physical reasonable SANCM outputs are obtainable only for restricted angular ranges.

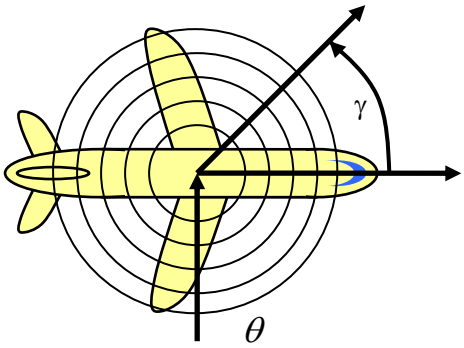

Figure 1: Azimuth-elevation plot, azimuth angle γ and elevation angle θ

Figure 2 shows the standard deviation and bias of the simulated pseudo-range error for the A340 aircraft. The presented simulation results are averaged over 30 approaches, whereas a resolution of 5 degree steps for azimuth and a resolution of 10 degree steps for elevation are used. To improve the statistics the two symmetry axes of the SANCM [19] are taken into account, resulting in 120 approaches per data point effectively. As expected, the delay error bias and variance generally decrease with an increasing elevation angle. A dependence on azimuth is less pronounced, but the most critical regions appear to be around ±45° and ±135°. It can also be seen that the error bias is much smaller than the standard deviation.

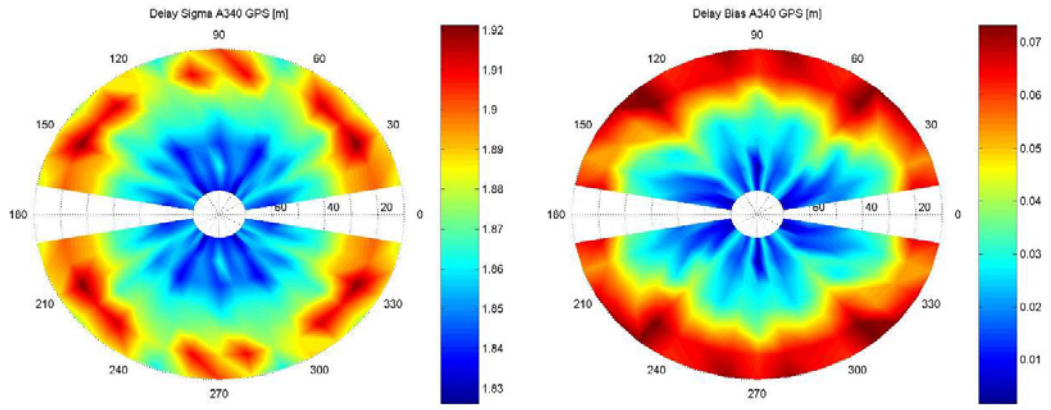

Figure 2: Standard deviation (left) and bias (right) over azimuth and elevation, aircraft A340

The results of the assessment reveal that the azimuth of the satellite constellation is not important while the elevation of the satellite plays the major role for the pseudo-range error distribution. Most critical pseudo-range errors are caused by the ground echo path. Due to variations of these echoes during an approach their contribution is not permanent. Instead, errors of extraordinarily high magnitude occur from time to time when the ground reflection has a severe influence [15]. Further investigations show that the pseudo-range error distribution is non-symmetric around the true pseudo-range (see Figure 3 and Figure 4, left figures respectively). Astonishingly, it is characterized by a long tail towards positive values. In the development of aircraft landing systems it is quite common to over bound the true error distribution by a wider Gaussian distribution. The results show that this over bounding distribution has a significantly larger standard deviation than the true standard deviation of the process. The knowledge of such over bounding distributions is very important for the certification of the final landing system.

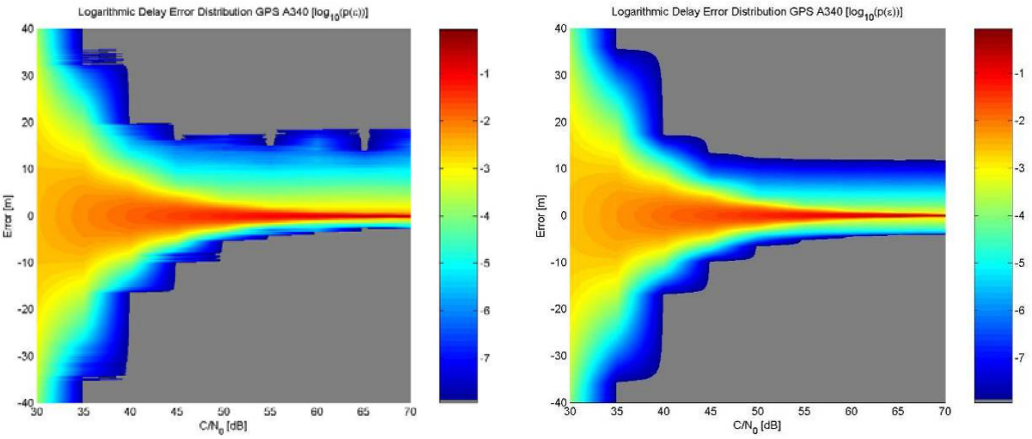

Figure 3: Comparison of pseudo-range error distributions for different C/N_0. Simulation (left) and calculation (right) .

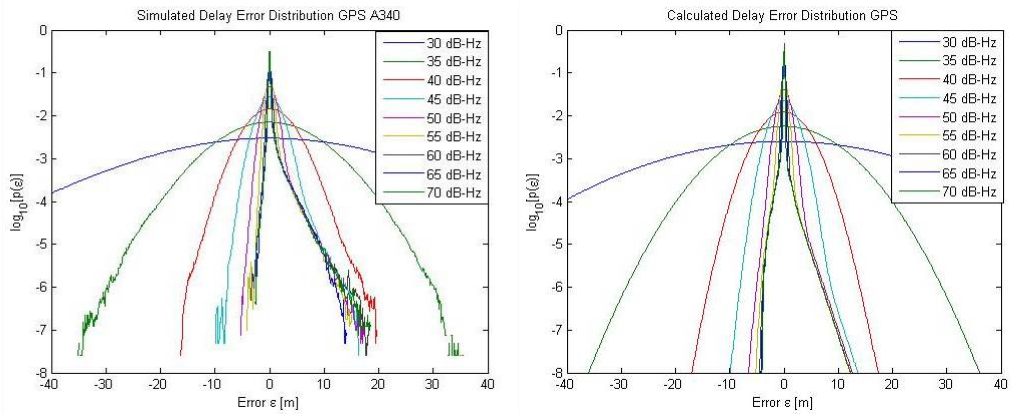

Figure 4: Comparison of pseudo-range error distributions for different C/N_0. Simulation (left) and calculation (right) .

To verify the simulation results a theoretical analysis based on the SANCM ground echo statistics was performed in [15], resulting in an analytical approximation of the pseudo-range error distribution (see Figure 3 and Figure 4, right figures respectively). Although these calculations can only give an approximation of the true error, the analysis serves as a valuable tool to explain and confirm the observations made from the simulation results.

GNSS Multipath Modelling in Urban Environments

Satellite navigation receivers are most challenged in urban environments. At first, the line-of-sight signal from certain satellites is often shadowed in urban canyons. Secondly, the satellite navigation radio signal is most often reflected, diffracted, and scattered on various objects like buildings, cars, trees, and lamp poles in city areas. DLR undertook high-resolution land mobile satellite channel (LMS) sounding measurements to investigate these effects which culminated in the development of highly realistic GNSS channel models for urban and suburban areas [12][16].

The channel was sounded at a frequency of 1.51 GHz and a bandwidth of 100MHz, resulting in a time resolution of 10 ns. The transmitter was mounted on a Zeppelin which served as vibration-poor hovering platform resembling a satellite. The Estimation of Signal Parameters via Rotational Invariance Techniques (ESPRIT) super-resolution algorithm was used to extrapolate the measured channel sounder data and to increase the resolution in time-domain.

The model comprises of a deterministic part with a generated scenery for calculating LOS signal shadowing and knife edge diffraction for house fronts, lamp poles, and tree trunks. The other observables like the number of coexisting echoes, the life span of reflectors, and the echoes' mean power are generated stochastically. Within the artificial scenery, every echo is initialized at a random position, the excess delays and Doppler phases for each echo are calculated geometrically. The measurements for the urban channel model were conducted in the Munich city center.

The main model assumption takes only multipath effects and receiver movement into account. The channel impulse response (CIR) $h(\Delta\tau, t)$ is expressed relative to the LOS signal and consists of N discrete echoes:

$$h(\Delta\tau, t) = \sum_{i=0}^{N} a_{r,i}(t) e^{-j\varphi_{r,i}(t)} \delta\left(\Delta\tau - \Delta\tau_i(t)\right)$$

where $a_{r,i}(t) = \frac{a_i(t)}{a_0(t)}$ denote the relative attenuation in terms of the direct signal path. The relative excess path delay is given by $\Delta\tau_i(t) = \tau_i(t) - \tau_0(t)$. The unobstructed LOS signal is represented by $a_{r,0}(t) = 1$ and $\Delta\tau_0(t) = 0$. $\varphi_{r,i}(t)$ represents phase variations dependent on receiver movement and the varying multipath environment.

An automatic recognition of start and stop times of single echoes from the ESPRIT-processed data was performed. Thus, the delay range, the life cycle, and the power distribution for each echo were determined. Additionally, the number of coexisting echoes could be calculated.

The inputs to the model define the scenery, the time-variant receiver speed and heading, and the satellite's azimuth and elevation. The model's output is a series of complex, time-variant channel impulse responses. Figure 5 shows an example for one CIR output.

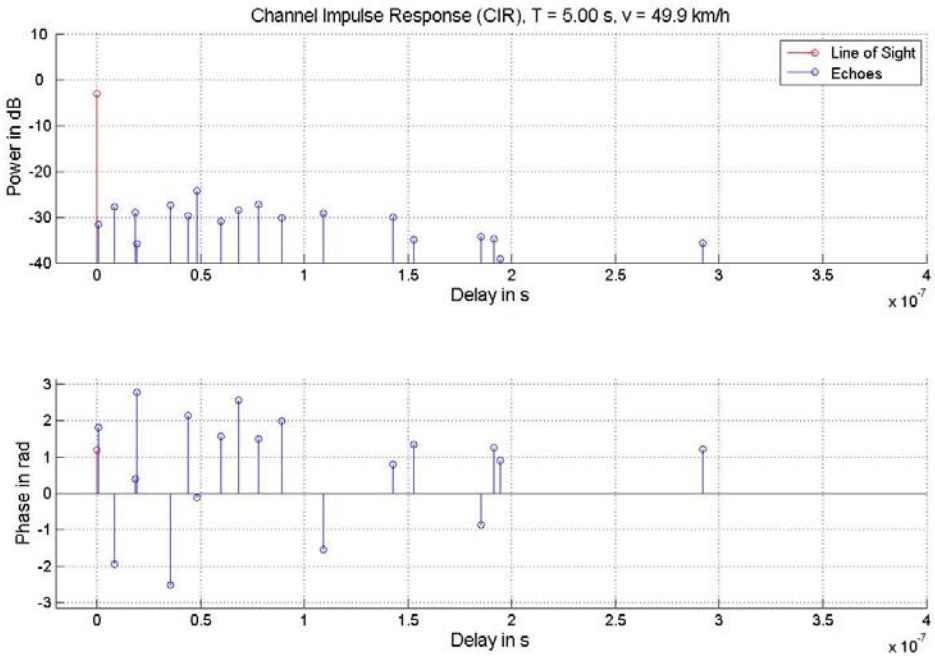

Figure 5: Output of the DLR LMS urban GNSS channel model. A single channel impulse response's magnitude and phase outputs are shown.

The model can be sampled at different rates, for the presented work, a CIR rate of R=1000 Hz was chosen. To fulfil the Nyquist Theorem regarding positive and negative Doppler, this CIR rate allows for a maximum vehicle speed of

$$v_{\max} = \frac{Rc_0}{2f_0} = \frac{1000\ \text{Hz} \cdot 3 \cdot 10^8\ \frac{\text{m}}{\text{s}}}{2 \cdot 1.51 \cdot 10^9\ \text{Hz}} = 100 \frac{\text{m}}{\text{s}}$$

with respect to stationary reflectors [11].

Realistic Simulation of GNSS reception in Urban Environments

Due to its realistic behaviour, the DLR urban model output comprises a high amount of drastically time-varying echoes. For the work on hand, echoes with a power of down to -100 dB with respect to LOS were taken into account. This led to a maximum of approximately 80 echoes in certain situations.

A simulation system which performs a sample-true simulation directly in the time-domain without using any simplifications has to perform the following tasks:

1. GPS signal generation
2. interface to channel model output: CIR time series
3. CIR to finite impulse response filter (FIR) coefficients interpolation
4. FIR filtering (convolution)
5. A/D conversion
6. software receiver module
    a. acquisition module
    b. tracking module and pseudo-range computation
7. evaluation tool to compare the convoluted signal to the undistorted signal.

The difficulty in simulating this chain lays in the bandwidth: For the GPS C/A code, a simulator sampling frequency of 40 MHz is being used in the presented work. The required filtering and channel convolution imposes a very high burden on the simulator software.

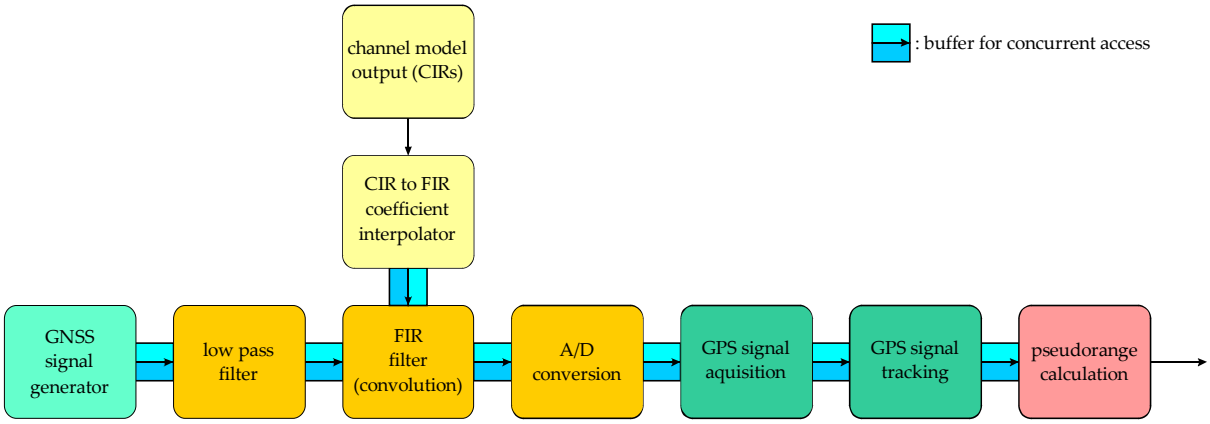

Figure 6: Structure of the newly developed sample-true GNSS simulation system.

A new high-efficient simulation system has been developed in C++ to perform pseudo-range simulations using the CIR output of highly realistic GNSS channel models. Figure 6 shows the general structure. Two implementation details made this GNSS sample-true simulation in a reasonable amount of time possible: Firstly, every module runs in an own thread. Thus, all threads are connected with circular buffers for concurrent access as shown in Figure 6. Secondly, performance-critical parts such as filtering, convolution, and correlation were optimized using Intel's SIMD (Single Instruction, Multiple Data) SSE2 instruction set. Yet, the program is still portable and compiles under Windows XP and Debian/GNU Linux. Figure 7 and Figure 8 show screenshots of the simulator software. Every column represent one signal processing module. The six modules in Figure 7 represent the following modules:

1. GPS signal generation
2. Low-pass filter
3. LMS urban channel model CIR output
4. CIR to FIR interpolation
5. convolution result
6. A/D conversion, sampling

The four columns in Figure 8 display the output of the software receiver module,

1. incoming signal's Is and Qs and the replica early, prompt, and late codes
2. I/Q plane, early, prompt, and late correlation results, pseudo-range computation
3. PLL and DLL output
4. correlation function, sampled at 13 instants.

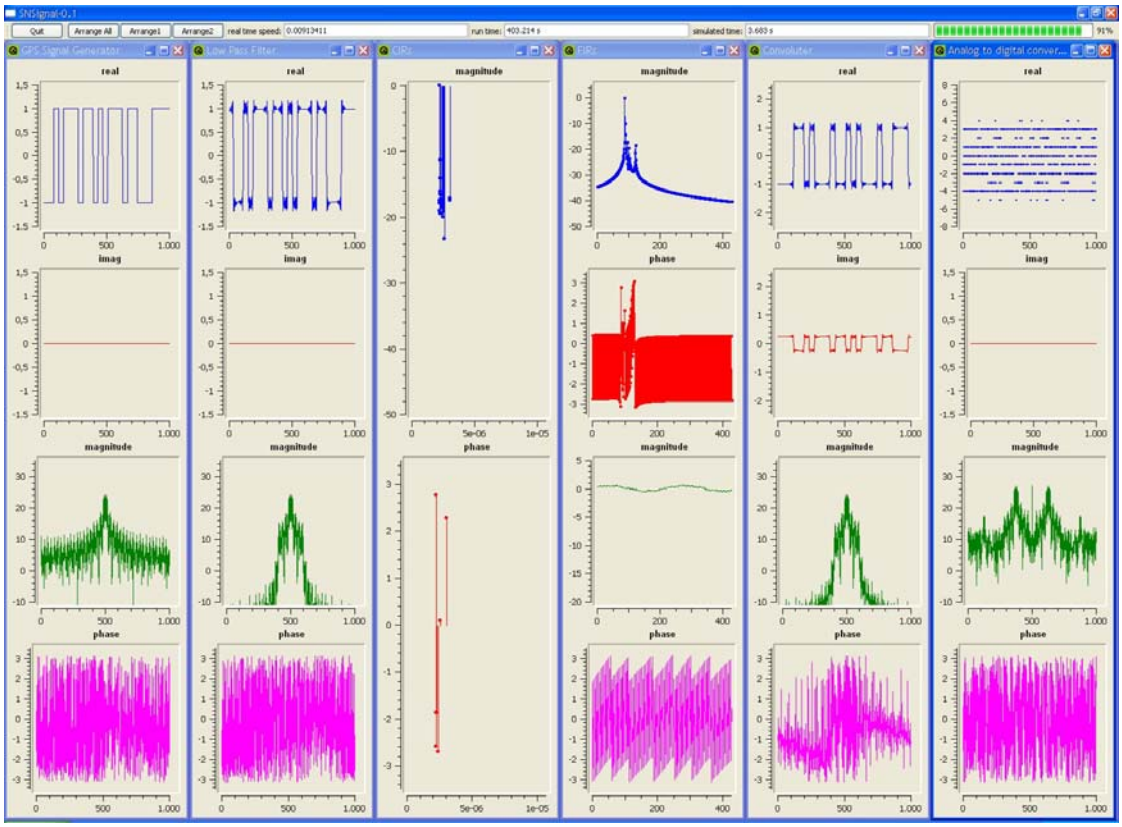

Figure 7: Simulator screenshot 1: signal generation, low-pass filtering, CIRs, FIRs, convolution result, up-conversion and sampling.

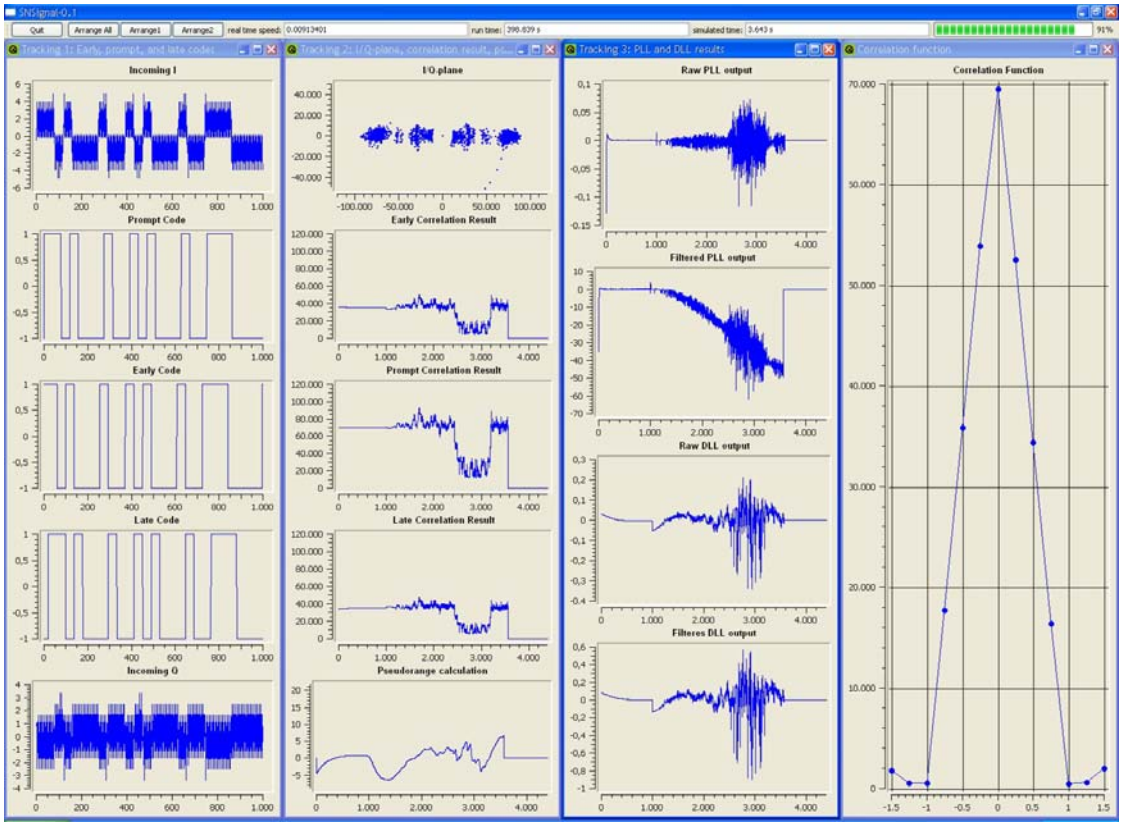

Figure 8: Simulator screenshot 2: code generation, tracking loop results, sampled correlation function, and pseudo-range result.

Design of Novel GNSS Receiver Multipath Mitigation Algorithms

An overview of multipath mitigation techniques is given in the following table. The left column represents the class of techniques that attempt to mitigate the effect of multipath in different ways. This can for example be achieved by modifications of the antenna response, either by means of hardware design or with signal processing techniques (e.g., beamforming). The majority of the remaining mitigation techniques are in some way aligning the more or less traditional receiver components (e.g., the early/late correlator) to the signal received in the multipath environment. To incorporate new signal forms (such as BOC), these methods need "tuning" in order to suffer as little as possible from multipath. On the other hand, multipath estimation techniques (right column) treat multipath (in particular the delay of the paths) as something to be estimated from the channel observations, so that its effects can be trivially removed at a later processing stage. For the estimation techniques, there are static and dynamic approaches, according to the underlying assumption of the channel dynamics. Examples for static multipath estimation are those belonging to the family of maximum likelihood (ML) estimators, often using different efficient maximization strategies over the likelihood function. For static channels without availability of prior information, the ML approach is optimal and performs significantly better than other techniques, especially if the echoes have short delay. Finally, dynamic estimators that target the computation of the posterior PDF conditioned on the received channel output sequence at the receiver can be applied.

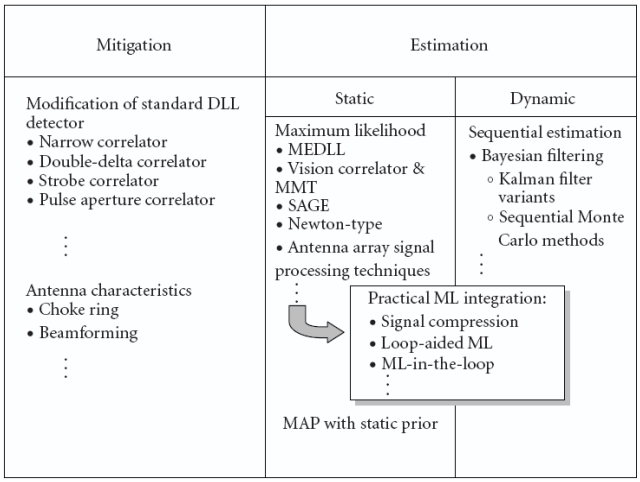

Table 1: Overview of multipath mitigation techniques

The classical mitigation techniques modify and shape the conventional early/late detector to reduce the impact of multipath. The narrow correlation [2] uses a conventional early/late correlator configuration, but their spacing is much smaller than one chip, e.g. 0.1 times the chip duration. This will be the reference mitigation method. The Double-Delta [3] correlator uses a pair of early/late correlators to form the loop-S curve detector.

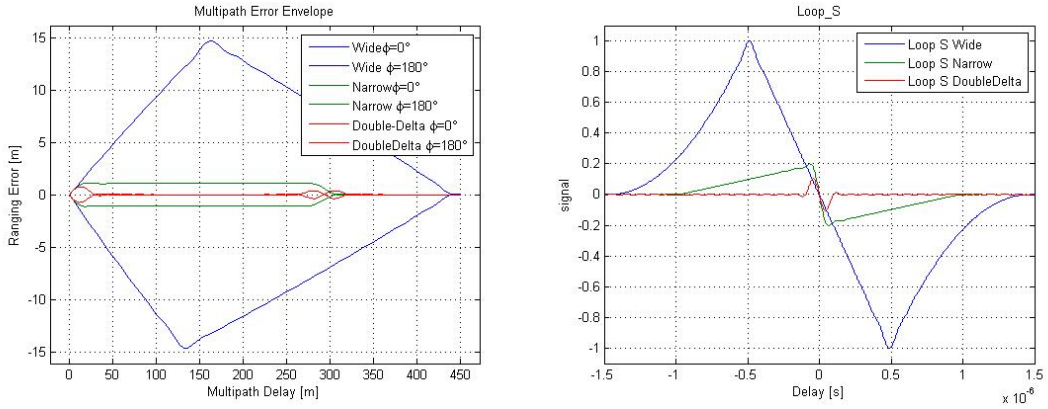

Figure 9: Multipath error envelope (left) and non-coherent loop-S detector curves (right) for the GPS L1 C/A signal with wide, narrow and double-delta correlator, signal-to-multipath ratio SMR=20dB

For the advanced mitigation techniques a signal parameter estimation problem is formulated, which takes the multipath replica explicitly into account. By considering the multipath in the signal model the formulation of an asymptotic efficient unbiased estimator is possible, such that the multipath bias is implicitly removed. Several strategies have been proposed in the literature to implement the ML estimator with low complexity [4], [6]. For the ML estimator the complex baseband signal model is a superposition of the LOS component and a specified number of replicas, whereas the sum of signals is assumed to be superimposed by white Gaussian noise:

$$z(t) = \sum_{i=1}^{N(t)} a_i(t) \cdot s(t - \tau_i(t)) + n(t)$$

where $z(t)$ is the received signal, $s(t)$ is the noise-free navigation signal, $a_i(t)$ are the complex amplitudes and $\tau_i(t)$ the delays of the respective paths, $N(t)$ is the number of paths and $n(t)$ the noise signal. The parameters are commonly assumed to be constant for a specific time interval. For this interval the signal is sampled and processed batch-wise. In vector notation the signal becomes

$$\mathbf{z} = \mathbf{S}(\boldsymbol{\tau})\mathbf{a} + \mathbf{n}$$

Given the Gaussian noise, the likelihood, namely the probability of the received signal conditioned on the signal parameters is maximized through a implementation-dependent method to obtain the ML estimates of the signal parameters:

$$\left\{\mathbf{a}^{ML}, \boldsymbol{\tau}^{ML}\right\} = \arg\max_{\mathbf{a},\boldsymbol{\tau}} p(\mathbf{z} \mid \mathbf{a}, \boldsymbol{\tau})$$

whereas $p(\mathbf{z}|\mathbf{a},\boldsymbol{\tau})$ is a complex Gaussian:

$$p(\mathbf{z}\,|\,\mathbf{a},\boldsymbol{\tau}) = \frac{1}{(2\pi)^L \sigma^L} \cdot \exp\left(-\frac{1}{2\sigma^2} (\mathbf{z} - \mathbf{S}(\boldsymbol{\tau})\mathbf{a})^H (\mathbf{z} - \mathbf{S}(\boldsymbol{\tau})\mathbf{a}) \right)$$

The length of the batch vector is L and the variance of the noise is σ^2. The unknown number of received paths N is obtained through a statistic test. Different path hypotheses are commonly compared based upon the estimation residual

$$\varepsilon(N) = \frac{1}{(2\pi)^L \sigma^L} \cdot \exp\left(-\frac{1}{2\sigma^2} (\mathbf{z} - \mathbf{S}(\boldsymbol{\tau}^{ML})\mathbf{a}^{ML})^H (\mathbf{z} - \mathbf{S}(\boldsymbol{\tau}^{ML})\mathbf{a}^{ML}) \right)$$

whereas higher order models commonly are penalized through the test metrics.

The a-posteriori minimum mean square error (MMSE) estimator [17], which is based on a particle filter implementation [5], is also a mitigation technique based on signal parameter estimation similar to the ML estimator. The difference of the two estimators is that the MMSE estimator is based on the concept of sequential Bayesian estimation. Estimates are not obtained independently for each time step, but rather at each time step prior knowledge that is derived from the past time steps is used to improve the quality of the estimates. Using the sequential Bayesian formulation the number of multipath signals can be estimated directly in terms of a random parameter, which is tracked along with the other signal parameters in a probabilistic fashion. To achieve this the signal model is extended by the binary random variable $e_i \in [1,0]$, which controls the activity of the paths:

$$z(t) = \sum_{i=1}^{N_{\max}} e_i(t) \cdot a_i(t) \cdot s(t - \tau_i(t)) + n(t)$$

Hence, in vector notation the signal for the observation period k becomes

$$\mathbf{z}_k = \mathbf{S}(\boldsymbol{\tau}_k)\mathbf{E}_k\mathbf{a}_k + \mathbf{n}$$

and the likelihood is thus

$$p(\mathbf{z}_k\,|\,\mathbf{e}_k,\mathbf{a}_k,\boldsymbol{\tau}_k) = \frac{1}{(2\pi)^L \sigma^L} \cdot \exp\left(-\frac{1}{2\sigma^2} (\mathbf{z}_k - \mathbf{S}(\boldsymbol{\tau}_k)\mathbf{E}_k\mathbf{a}_k)^H (\mathbf{z}_k - \mathbf{S}(\boldsymbol{\tau}_k)\mathbf{E}_k\mathbf{a}_k) \right)$$

To estimate the posterior distribution $p(\mathbf{e}_k,\mathbf{a}_k,\boldsymbol{\tau}_k|\mathbf{Z}_k)$, $\mathbf{Z}_k=\{\mathbf{z}_0,..,\mathbf{z}_k\}$, the likelihood is joined with a prior density $p(\mathbf{e}_k,\mathbf{a}_k,\boldsymbol{\tau}_k\,|\,\mathbf{Z}_{k-1})$, which introduces the prior knowledge about the parameters:

$$p(\mathbf{e}_k,\mathbf{a}_k,\boldsymbol{\tau}_k\,|\,\mathbf{Z}_k) = C \cdot p(\mathbf{z}_k\,|\,\mathbf{e}_k,\mathbf{a}_k,\boldsymbol{\tau}_k) \cdot p(\mathbf{e}_k,\mathbf{a}_k,\boldsymbol{\tau}_k\,|\,\mathbf{Z}_{k-1})$$

The prior density, which is not considered by the ML estimator, is obtained from the previous posterior through a prediction step, which follows

$$p(\mathbf{e}_k, \mathbf{a}_k, \boldsymbol{\tau}_k \mid \mathbf{Z}_{k-1}) =$$
$$\int_{\mathbf{e}_{k-1}, \mathbf{a}_{k-1}, \boldsymbol{\tau}_{k-1}} p(\mathbf{e}_k, \mathbf{a}_k, \boldsymbol{\tau}_k \mid \mathbf{e}_{k-1}, \mathbf{a}_{k-1}, \boldsymbol{\tau}_{k-1}) p(\mathbf{e}_{k-1}, \mathbf{a}_{k-1}, \boldsymbol{\tau}_{k-1} \mid \mathbf{Z}_{k-1}) d\mathbf{e}_{k-1} d\mathbf{a}_{k-1} d\boldsymbol{\tau}_{k-1}$$

which makes use of the statistical dependencies between successive observation intervals through the transition density $p(\mathbf{e}_k,\mathbf{a}_k,\boldsymbol{\tau}_k|\mathbf{e}_{k-1},\mathbf{a}_{k-1},\boldsymbol{\tau}_{k-1})$. The MMSE estimate is then given by

$$\begin{aligned} \boldsymbol{\tau}^{MMSE} &= \int_{\boldsymbol{\tau}_k, \mathbf{e}_k, \mathbf{a}_k} \boldsymbol{\tau}_k \cdot p(\mathbf{e}_k, \mathbf{a}_k, \boldsymbol{\tau}_k \mid \mathbf{Z}_k) d\mathbf{e}_k d\mathbf{a}_k d\boldsymbol{\tau}_k \\ &= \int_{\boldsymbol{\tau}_k} \boldsymbol{\tau}_k \cdot p(\boldsymbol{\tau}_k \mid \mathbf{Z}_k) d\boldsymbol{\tau}_k \end{aligned}$$

Since the sequential approach takes benefit of the temporal correlation of the channel, future sequential algorithms can take advantage of highly realistic channel models, as actually the task of channel modelling comes close to the development of a proper characterization of the temporal channel statistics through the transition density $p(\mathbf{e}_k,\mathbf{a}_k,\boldsymbol{\tau}_k|\mathbf{e}_{k-1},\mathbf{a}_{k-1},\boldsymbol{\tau}_{k-1})$. In fact, given a channel model is characterized through a Markovian process that follows the transition PDF $p(\mathbf{e}_k,\mathbf{a}_k,\boldsymbol{\tau}_k|\mathbf{e}_{k-1},\mathbf{a}_{k-1},\boldsymbol{\tau}_{k-1})$, the optimal sequential algorithm will use the same density to compute the prior PDF $p(\mathbf{e}_k,\mathbf{a}_k,\boldsymbol{\tau}_k|\mathbf{Z}_{k-1})$. Thus there are two major benefits for designing future advanced mitigation algorithms: On the one hand the statistical model underlying the mitigation algorithm can be adapted and trained to fit the model statistics, and on the other hand the novel algorithm can be verified when being exposed to the model.

Simulation runs

To assess the performance of the MMSE multipath mitigation algorithm, three procedures could be applied:

1. Generate GNSS signals with a fixed amount of predetermined multipath disturbances, i.e. the direct path plus one or two discrete echoes. This procedure can serve as a verification of the algorithm's capability of tracking discrete echoes but it does not provide an insight into its behaviour in realistic environments.
2. Direct use of CIR measurement data from the DLR urban environment measurement campaign. A disadvantage is the limited availability of measurement data and the limited amount of measured scenarios.
3. Usage of the DLR LMS GNSS channel model. This allows for a statistical analysis of the algorithm's performance behaviour due to the possibility of long simulation runs for many different scenarios (regarding the satellite's position and the user vehicle trajectory).

Assessment of Navigation Signals under Realistic Conditions Using Measured CIRs

The complexity of a mobile urban navigation channel is shown in Figure 10. Various situations challenge the mitigation algorithm simultaneously: Dynamic LOS blockage and shadowing as well as appearing and disappearing multipath signals.

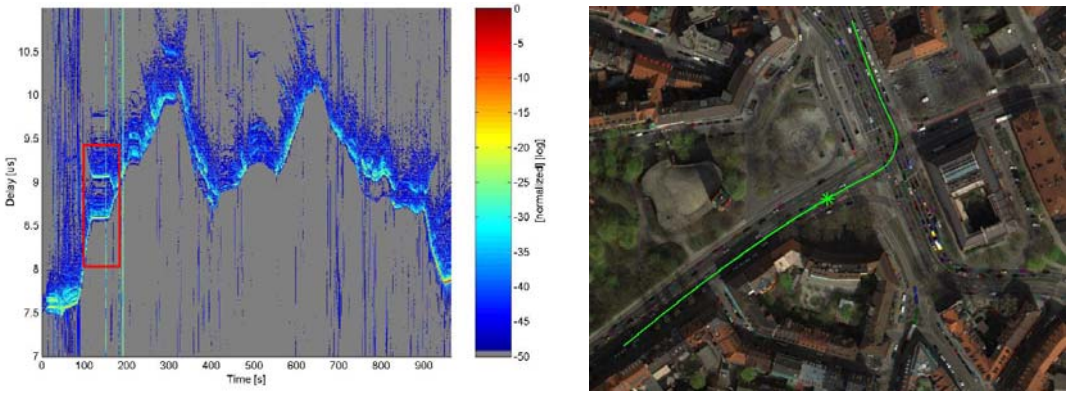

Figure 10: Measurement of urban navigation channel in Munich (left). The section highlighted by the box corresponds to a stop of the vehicle at a traffic light. The position of the stop is indicated by the marker on the track (right).

Figure 11 shows how a dynamic mitigation algorithm is able to cope with these situations. Where conventional tracking algorithms fail, the sequential algorithm is able to detect and track the appearing multipath signal, which implicitly removes the multipath errors on the LOS estimate. As illustrated the bandwidth of the channel fading process is smaller than the tracking bandwidth of the loop during the selected stop period, since the DLL is not able to average out the multipath errors. The multipath-induced time-variant tracking error is reduced significantly by smoothing the DLL estimate with carrier measurements. If reliable tracking of the phase is not available, the carrier smoothing obviously fails (t > 60s). For the MMSE estimator the tracking estimate remains accurate, independent of the carrier tracking performance.

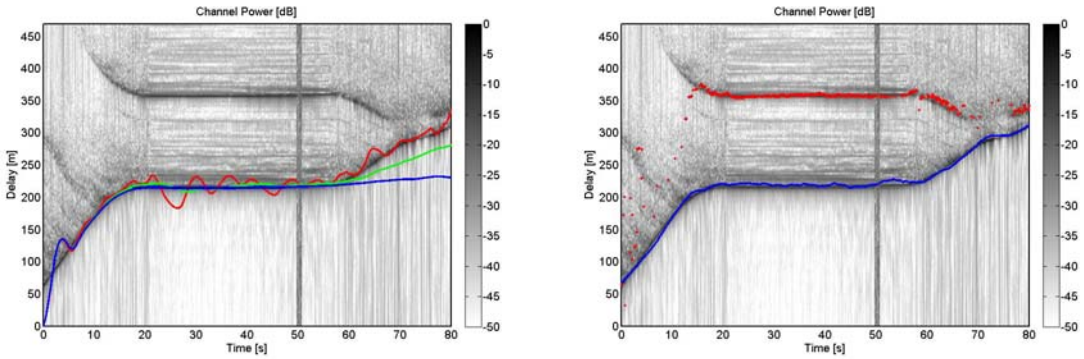

Figure 11: DLL tracking for the previously highlighted channel section (left). Narrow correlator (red), with 10s (green) and 100s (blue) carrier smoothing. MMSE estimator (right) with LOS estimate (blue) and multipath track (red).

The simulation of highly realistic channels is also valuable for the assessment of the multipath mitigation capabilities of novel navigation signals. Commonly these assessments are performed for static channel configurations and standard receiver implementations, which are useful for obtaining first hints on the expectable performance, but which give only limited insight finally, in particular with respect to novel dynamic mitigation algorithms. Figure 12 shows the results of a simulation stimulated by a measured vehicular and pedestrian channel scenario with a BPSK and a BOC(1,1) [8] modulated signal respectively when using different types of mitigation algorithms. The results are summarized in Table 2.

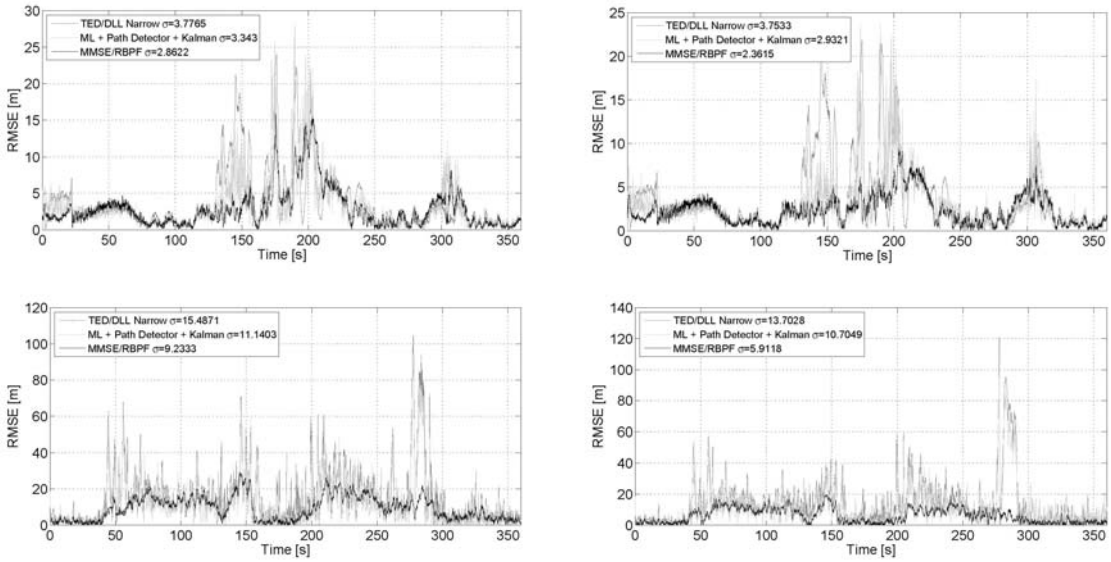

Figure 12: Magntiude of time-delay estimation error over time for vehicular (top) and pedestrian scenario. BPSK signal (left) and BOC(1,1) signal (right).

BPSK / BOC(1,1)	*Pedestrian*	*Vehicular*
DLL/TED	15.5m / 13.7m	3.8m / 3.7m
ML+Kalman	11.1m / 10.7m	3.3m / 2.9m
MMSE	9.2m / 5.9m	2.9m / 2.4m

Table 2: Summary of algorithm performance depending on user scenario and navigation signal

Even if the advance in average performance is rather small the results show that the more advanced algorithms are more robust against exceptional error events, which arise occasionally during LOS blockage and shadowing periods. The results confirm also that the channel statistics itself can have much more impact on the performance than the shape of the navigation signal. Figure 13 illustrates the behaviour of the Bayesian MMSE algorithm in some typical urban/sub-urban multipath scenarios.

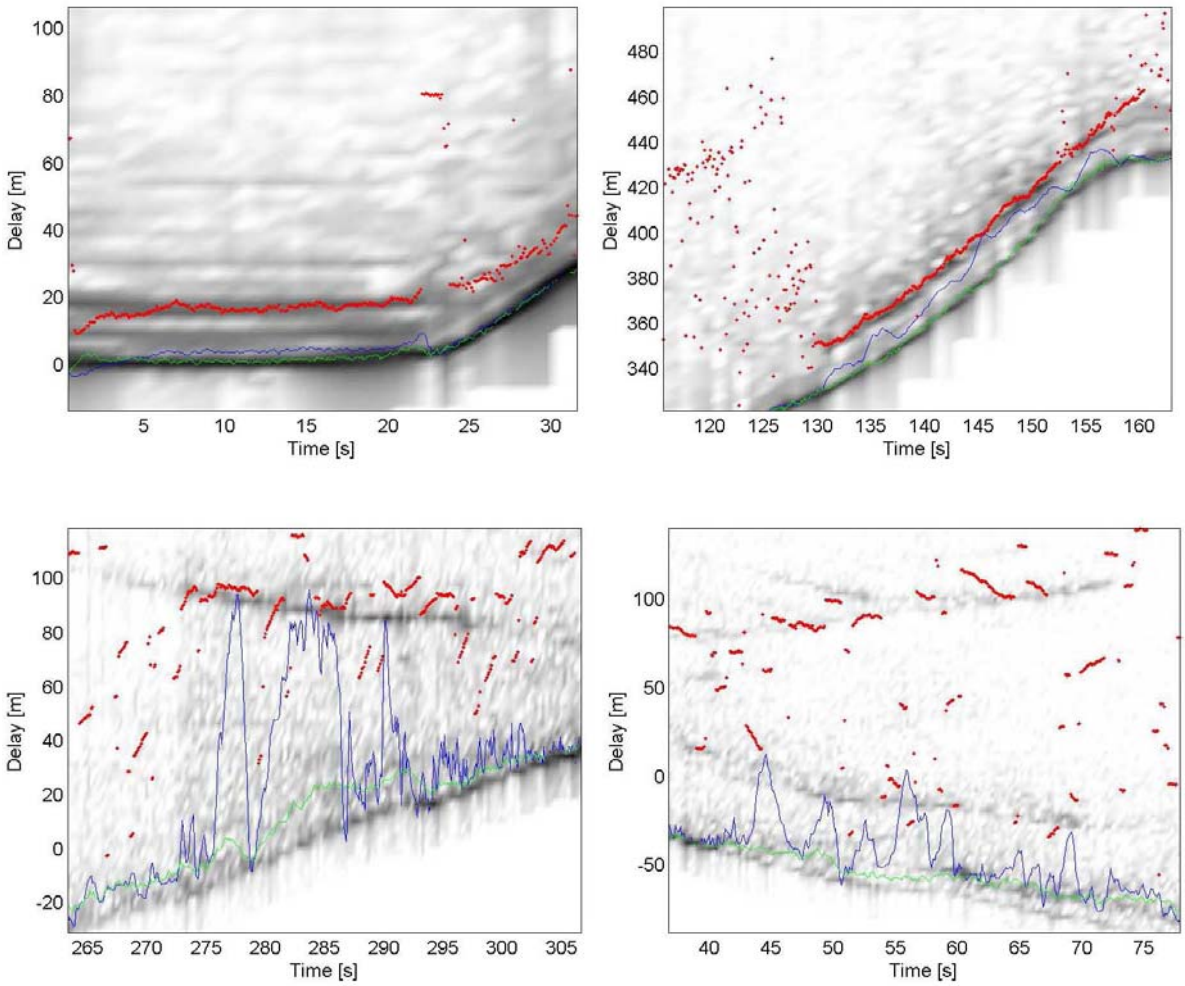

Figure 13: Bayesian MMSE estimator in comparison with DLL under typical multipath scenarios. DLL estimate (blue), MMSE LOS estimate (green), and MMSE multipath estimates (red). Top-left: Capturing and tracking a close-in static multipath replica. Top-right: Tracking a multipath replica during movement. Bottom-left: Coping with multiple simultaneous replica. Bottom-right: Bridging through a shadowed LOS superimposed by strong multipath.

Assessment of Navigation Signals under Realistic Conditions Using the DLR LMS GNSS Urban Channel Model

The results of a 120s simulation run are presented. The parameters of the simulation parameters are listed in Table 3. In the simulation, the satellite was positioned at an elevation of 25° and an azimuth of 135°, i.e. the vehicle was moving away from the satellite. The maximum speed was 50 km/h and 3 full stops were included in the vehicle's trajectory.

Sampling frequency	40 Hz
Intermediate frequency	5 MHz

ADC resolution	4 bit
early-late spacing	1 chip
PLL damping ratio	0.7
PLL noise bandwidth	25 Hz
PLL discriminator	$\varphi = \tan^{-1}\left(\frac{Q^k}{I^k}\right)$
DLL damping ratio	0.7
DLL noise bandwidth	2 Hz
DLL discriminator	$D = \frac{(I_E^{\,2} + Q_E^{\,2}) - (I_L^{\,2} + Q_L^{\,2})}{(I_E^{\,2} + Q_E^{\,2}) + (I_L^{\,2} + Q_L^{\,2})}$

Table 3: Simulation parameters

A GPS C/A code signal was generated, low-pass filtered to 4 MHz and convoluted with the channel impulse responses at the respective moments using the above mentioned newly developed GNSS simulator software. The correlation function was sampled at 13 equally spaced instants starting from -1.5 chips to 1.5 chips in 0.25 chips steps.

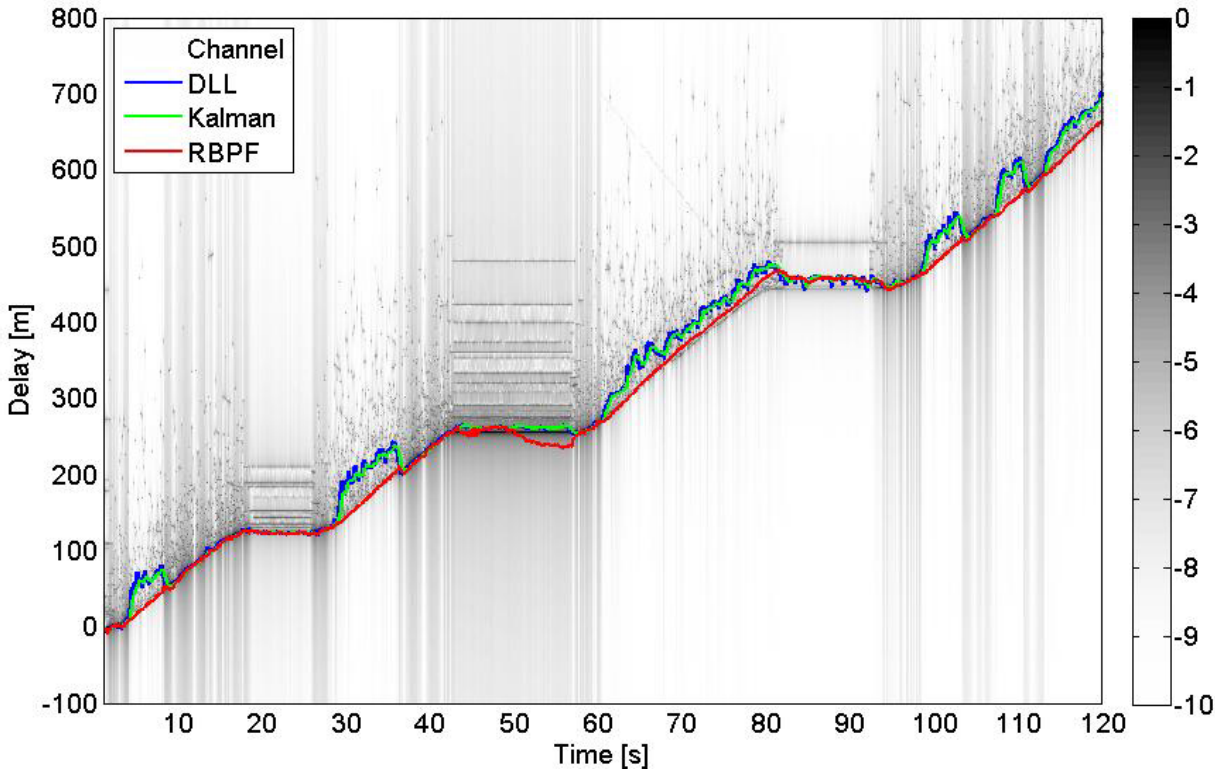

Figure 14: 120s run of a realistic urban scenario with periods of shadowed and direct LOS operation. Performance of DLL (blue), Kalman filter (green), and Bayesian MMSE estimator (red).

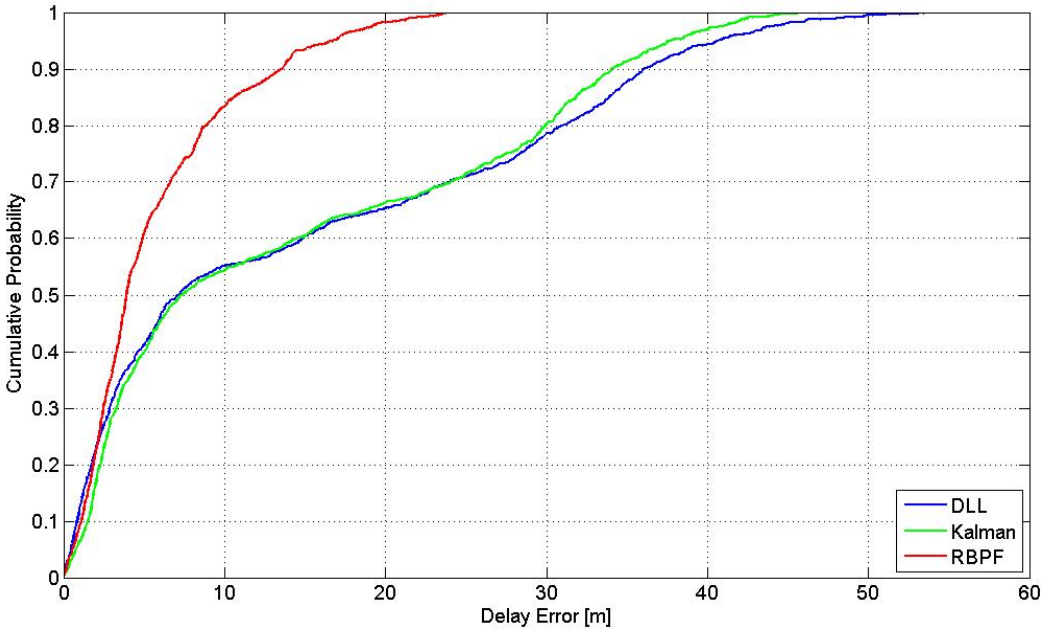

Figure 15: Normalized cumulative error histogram corresponding to the results shown in Figure 14.

Conclusion

In this paper we have shown several applications for the simulation of high-realistic multipath environments and recent developments in the area of simulation tools and signal processing algorithms for navigation receivers. Measured as well as artificial channel data, as it can be generated by novel high-realistic channel models, have been shown to be valuable for the development and assessment of navigation signals and future receiver algorithms. The results confirm that significant advance may be expected from future sophisticatedly shaped navigation signals and novel signal processing algorithms.

References

[1] E. D. Kaplan, Ed., (1996): Understanding GPS: Principles and Applications Boston, London: Artech House Publishers, 1996.

[2] A. van Dierendonck, P. Fenton, and T. Ford, (1992): “Theory and performance of narrow correlator spacing in a GPS receiver,” in Proceedings of the National Technical Meeting of the Satellite Division of the Institute of Navigation (ION NTM 1992), San Diego, California, USA

[3] L. Garin, F. van Diggelen, and J.-M. Rousseau, (1996): “Strobe and edge correlator multipath mitigation for code,” in Proceedings of the 9th International Technical Meeting of the Satellite Division of the Institute of Navigation (ION GPS 1996), Kansas City, Montana, USA

[4] D. van Nee, J. Siereveld, P. Fenton, and B. Townsend, (1994): "The multipath estimating delay lock loop: Approaching theoretical accuracy limits," in Proceedings of the IEEE Position Location and Navigation Symposium (PLANS 94), Las Vegas, Nevada, USA

[5] S. Arulampalam, S. Maskell, N. Gordon, and T. Clapp, (2002): "A tutorial on particle filters for online nonlinear/non-Gaussian Bayesian tracking," IEEE Transactions on Signal Processing, vol. 50, no. 2, pp. 174–188, Feb. 2002.

[6] J. Selva, (2005) "An efficient Newton-type method for the computation of ML estimators in a uniform linear array," IEEE Transactions on Signal Processing, vol. 53, no. 6, pp. 2036–2045, June 2005.

[7] M. Irsigler, G. Hein, and B. Eissfeller, (2004) "Multipath performance analysis for future GNSS signals," in Proceedings of the National Technical Meeting of the Satellite Division of the Institute of Navigation (ION NTM 2004), San Diego, California, USA

[8] J. Avila-Rodriguez, G. Hein, S. Wallner, J. Issler, L. Ries, L. Lestarquit, A. De Latour, J. Godet, F. Bastide, T. Pratt, and J. Owen, (2007) "The MBOC modulation: The final touch to the Galileo frequency and signal plan," in Proceedings of the 20th International Technical Meeting of the Satellite Division of the Institute of Navigation (ION GNSS 2007), Fort Worth, Texas, USA

[9] Steingass, A.; Lehner, A.; Fontan, F.; Kubista, E.; Martin, M.J.; Arbesser-Rastburg, B. (2004): "A High Resolution Model for the Aeronautical channel" in Proceedings of the PLANS 2004, Proceedings of the 2004 IEEE Position, Location and Navigation Symposium (PLANS 2004), Coronado, California, USA

[10] Steingass, Alexander; Lehner, Andreas (2004): "Measuring the Navigation Multipath Channel: A Statistical Analysis," Proceedings of the 17th International Technical Meeting of the Institute of Navigation Satellite Division (ION GNSS 2004), Long Beach, California, USA

[11] Lehner, Andreas: "Multipath Channel Modelling for Satellite Navigation Systems", Shaker Verlag, 2007. PhD thesis.

[12] Lehner, Andreas; Steingass, Alexander (2005): "A Channel Model for land mobile satellite navigation," in Proceedings of the 18th International Technical Meeting of the Institute of Navigation Satellite Division (ION GNSS 2005), Long Beach, California, USA

[13] Lentmaier, Michael; Krach, Bernhard (2006): "Maximum Likelihood Multipath Estimation in Comparison with Conventional Delay Lock Loops," in Proceedings of the 19th International Technical Meeting of the Institute of Navigation Satellite Division (ION GNSS 2006), Fort Worth, Texas, USA

[14] Macabiau, C., Moriella, L., Raimondi, M., Dupouy, C., Steingaß, A., Lehner, A.: "GNSS Airborne Multipath Errors Distribution Using the High Resolution Aeronautical Channel Model and Comparison to SARPs Error Curve," in Proceedings of the Institute of Navigation National Technical Meeting (ION NTM 2006), Monterey, California, USA

[15] Lentmaier, Michael; Krach, Bernhard; Jost, Thomas; Lehner, Andreas; Steingass, Alexander (2007): "Assessment of Multipath in Aeronautical Environments," Proceedings of the 2007 European Navigation Conference (ENC-GNSS 2007), Geneva, Switzerland

[16] Steingass, Alexander; Lehner, Andreas (2007): "Navigation in Multipath Environments for Suburban Applications," in Proceedings of the 20th International Technical Meeting of the Institute of Navigation Satellite Division (ION GNSS 2007), Fort Worth, Texas, USA

[17] Lentmaier, Michael; Krach, Bernhard; Robertson, Patrick; Thiasiriphet, Thanawat (2007): "Dynamic Multipath Estimation by Sequential Monte Carlo Methods," in Proceedings of the 20th International Technical Meeting of the Institute of Navigation Satellite Division (ION GNSS 2007), Fort Worth, Texas, USA

[18] Krach, Bernhard; Lentmaier, Michael; Robertson, Patrick (2008): "Joint Bayesian Positioning and Multipath Mitigation in GNSS," in Proceedings of the 2008 IEEE International Conference on Acoustics, Speech, and Signal Processing (ICASSP 2008), Las Vegas, Nevada, USA

[19] Steingass, Alexander; Lehner, Andreas; Pérez-Fontán, Fernando; Kubista, Erwin; Arbesser-Rastburg, Bertram (2008): "Characterization of the aeronautical satellite navigation channel through high-resolution measurement and physical optics simulation," International Journal of Satellite Communications and Networking (26), John Wiley & Sons, Ltd., S. 1 - 30, DOI 10.1002/sat.891

[20] Lentmaier, Michael; Krach, Bernhard; Robertson, Patrick (2008): "Bayesian Time Delay Estimation of GNSS Signals in Dynamic Multipath Environments," International Journal of Navigation and Observation, Hindawi Publishing Corporation, DOI 10.1155/IJNO, ISSN 1687-5990

[21] ITU Recommendation ITU-R 682-2 (2007): "Propagation Data Required for the Design of Earth-Space Aeronautical Mobile Telecommunication Systems", International Telecommunication Union, Geneva, 2007.